Original Article Clinics in Orthopedic Surgery 2024;16:493-505 • https://doi.org/10.4055/cios23376

Anterolateral Dual Plate Fixation for Distal Metaphyseal-Diaphyseal Junction Fractures of the Humerus: Biomechanical Finite Element Analysis with Clinical Results

Cheungsoo Ha, MD, Inrak Choi, PhD*, Jun-Ku Lee, MD†, Jongbeom Oh, MD, Wooyeol Ahn, MD, Soo-Hong Han, MD

Department of Orthopaedic Surgery, CHA Bundang Medical Center, CHA University School of Medicine, Seongnam, Korea
**Intuitive Surgical Inc., Sunnyvale, CA, USA*
†Department of Orthopaedic Surgery, National Health Insurance Service Ilsan Hospital, Goyang, Korea

Background: Distal metaphyseal-diaphyseal junction fractures of the humerus are a subset of injuries between humeral shaft fractures and distal intra-articular humerus fractures. A lack of space for distal fixation and the unique anatomy of concave curvature create difficulties during operative treatment. The closely lying radial nerve is another major concern. The aim of this study was to determine whether anterolateral dual plate fixation could be effective for a distal junctional fracture of the humerus both biomechanically and clinically.

Methods: A right humerus 3-dimensional (3D) model was obtained based on plain radiographs and computed tomography data of patients. Two fractures, a spiral type and a spiral wedge type, were constructed. Three-dimensional models of locking compression plates and screws were constructed using materials provided by the manufacturer. The experiment was conducted by using COMSOL Multiphysics, a finite element analysis, solver, and simulation software package. For the clinical study, from July 2008 to March 2021, a total of 72 patients were included. Their medical records were retrospectively reviewed to obtain patient demographics, elbow range of motion, Disabilities of the Arm, Shoulder and Hand (DASH) scores, Mayo Elbow Performance Scores (MEPS), and hand grip strength.

Results: No fracture fixation construct completely restored stiffness comparable to the intact model in torsion or compression. Combinations of the 7-hole and 5-hole plates and the 8-hole and 6-hole plates showed superior structural stiffness and stress than those with single lateral plates. At least 3 screws (6 cortices) should be inserted into the lateral plate to reduce the load effectively. For the anterior plate, it was sufficient to purchase only the near cortex. Regarding clinical results of the surgery, the range of motion showed satisfactory results in elbow flexion, elbow extension, and forearm rotation. The average DASH score was 4.3 and the average MEPS was 88.2.

Conclusions: Anterolateral dual plate fixation was biomechanically superior to the single-plate method in the finite element analysis of a distal junctional fracture of the humerus model. Anterolateral dual plate fixation was also clinically effective in a large cohort of patients with distal junctional fractures of the humerus.

Keywords: *Finite element analysis, Biomechanics, Computational modelling, Humeral fractures, Clinical outcome*

Received November 22, 2023; Revised December 18, 2023; Accepted December 18, 2023
Correspondence to: Soo-Hong Han, MD
Department of Orthopaedic Surgery, CHA Bundang Medical Center, CHA University School of Medicine, 59 Yatap-ro, Bundang-gu, Seongnam 13496, Korea
Tel: +82-31-780-5270, Fax: +82-31-708-3578, E-mail: hsoohong@cha.ac.kr
Cheungsoo Ha and Inrak Choi contributed equally to this article as co-first authors.

Humeral shaft fractures accunt for approximately 3% of all fractures and 20% of all fractures involving the humerus.[1] In an epidemiologic study of 249 consecutive humeral shaft fractures in the United Kingdom, 10% of humeral diaphyseal fractures occurred in the distal metaphyseal diaphyseal junction.[2] Distal metaphyseal-diaphyseal junction fractures of the humerus (DJFHs) seem to be another subset of injuries between humeral shaft fractures and distal intra-articular humerus fractures.

Most simple midshaft fractures of the humerus are traditionally treated nonsurgically.[3] However, some surgeons prefer a surgical approach due to higher risks of nonunion, malalignment, and decreased elbow function associated with nonsurgical methods.[4,5] Many orthopedic surgeons recommend open reduction and internal fixation to manage midshaft humerus fractures. For distal intra-articular fractures, dual plating has been frequently chosen based on the 2-column theory.[6] However, there is no standard or universal treatment option for DFJHs.

Due to the lack of space for distal fixation and the unique anatomy of concave curvature, DJFHs are considered more challenging to treat than other humerus fractures.[7,8] The closely lying radial nerve is another major concern.[9] Several methods have been proposed to overcome surgical difficulties.[10-12] However, the gold standard surgical fixation technique or approach for DJFHs is still debatable.

Recent efforts have been made to operate on DJFHs using anterolateral dual plate fixation (ADPF).[7,13] Previous clinical studies have suggested that compared to existing lateral single-plate fixation methods, ADPF is a promising surgical method for DJFHs by increasing the treatment effectiveness without significantly altering the incision site or operation time. However, the results of the previous studies were limited to a small number of patients, and supportive biomechanical studies were insufficient to demonstrate the efficacy of ADPF.

Advancements in computer-based simulation and analytical research techniques have provided more information on biomechanical understanding. Finite element analysis (FEA) is one of the most popular tools and is gradually increasing in fracture fixation studies.[14] A past FEA study has shown that dual plate fixation can be effective in the humerus.[15] However, this study was conducted with limited controlled parameters and did not realistically consider the shape of the humerus or the fracture type in the lower part of the humerus.

Thus, we simultaneously performed a biomechanical study using FEA and a clinical study using an extended large-number cohort. The aim of this study was to determine whether ADPF could be effective biomechanically and clinically for DJFHs. Specifically, the FEA study was conducted to determine the effectiveness of ADPF by considering various control parameters with more realistic fracture models.

METHODS

This study was approved by Institutional Review Board of CHA Bundang Medical Center and the local Ethics Committee (IRB No. 2022-04-075). The requirement for informed consent was waived due to the retrospective nature of this study; however, consent for using the images was obtained from the patients.

Finite Element Analysis

Experiment design

FEA experiments were designed with multiple control parameters to address several questions encountered during a surgery. First, a main experiment was planned to determine whether ADPF could more effectively resist loads than the lateral single plate fixation, which is a typical surgical method for DJFHs. Second, an experiment was planned to determine whether there was a difference in biomechanical performance according to the lengths of the plates for ADPF. Lastly, an experiment was conducted to investigate whether there was a biomechanical difference according to the number of cortices purchased. To answer these questions, we considered 2 types of fractures: spiral and spiral wedge types.

A total of 8 models were designed, and the control parameters for each model are indicated in Table 1. The comparison of models A and B and that of models D and E examined the effectiveness of ADPF in the 2 types of fractures. The comparison of models B and C and that of models E and F were to show the effect of the lengths of

Table 1. The Control Parameters of the 8 Three-dimensional Models and Their Fixation Methods

Model	Fracture classification	Lateral plate	Anterior plate	Fixation method
A	AO 12-B1	4.5 Plate 7-hole	None	For the lateral plate, cortical screws were used in the 1st, 3rd, 5th, and 7th holes, and locking screws were used in the 2nd and 6th holes.
B	AO 12-B1	4.5 Plate 7-hole	Plate 5-hole	For the lateral plate, the same method used for model A was used. For the anterior plate, cortical screws were used in the 1st and 5th holes, and locking screws were used in the 2nd and 4th holes. All screws are installed unicortically.
C	AO 12-B1	Plate 8-hole	3.5 Plate 6-hole	For the lateral plate, cortical screws were used in the 1st, 3rd, 6th, and 8th holes, and locking screws were used in the 2nd and 7th holes. For the anterior plate, cortical screws were used in the 1st and 6th holes, and locking screws were used in the 2nd and 5th holes. All screws are installed unicortically.
D	AO 12-A1	4.5 Plate 7-hole	None	Identical to model A
E	AO 12-A1	4.5 Plate 7-hole	3.5 Plate 5-hole	Identical to model B
F	AO 12-A1	4.5 Plate 8-hole	3.5 Plate 6-hole	Identical to model C
G	AO 12-A1	4.5 Plate 7-hole	3.5 Plate 5-hole	Identical to model E except that there are no cortical screws in the 3rd and 5th holes of the lateral plate.
H	AO 12-A1	4.5 Plate 7-hole	3.5 Plate 5-hole	Identical to model E except that all screws in the anterior plate are installed bicortically.

the plates used for ADPF. The comparison between models E and G was to show the effect of the number of screws used in the lateral plate on the biomechanical performance of ADPF. The comparison between models E and H was to investigate the performance difference due to the unicortical and bicortical screw fixation methods of the acterior plate. The actual models used in the simulation environments are shown in Fig. 1.

Three-dimensional modeling

Three-dimensional (3D) models for FEA were implemented with Solidworks, a computer-aided design software program (Education Edition 2019-2020, Dassault Systems). The 3D model of the right humerus was obtained from BodyParts3D, an open-source 3D structure database.[16] This humerus model was made of a 2 mm-thick cortical bone. Two types of fractures, a spiral fracture (AO type 12-A1) and a spiral wedge fracture (AO type 12-B1), were constructed based on plain radiographs and computed tomography (CT) data of patients. Fig. 2 displays the constructed models along with the corresponding CT images. Both fractures were located in the lower third of the humerus.

The 3D models of locking compression plates (LCPs) and screws were created based on the designs and the materials provided by the manufacturer (DePuy Synthes). For implantation in the lateral part of the humerus, 7-hole and 8-hole 4.5-mm narrow LCPs were used. The plates

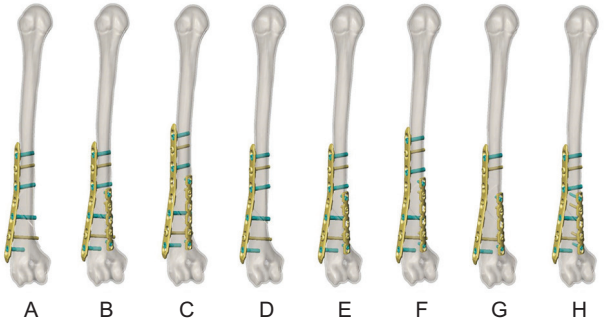

Fig. 1. Various 3-dimensional models and their parameters. Table 1 shows detailed conditions.

were bent by 10° between the third and fourth holes and between the fourth and fifth holes, respectively, to match the shape of the humerus. For the anterior part of the humerus, 5-hole and 6-hole 3.5-mm reconstruction plates were used. Self-tapping locking screws and cortical screws suitable for each experimental condition were designed as cylindrical shapes with the same diameter as the actual models. The screws were then attached to the plates as shown in Fig. 1. The number and arrangement of the locking screws and cortical screws used in each model are described in Table 1.

In both fracture models, the bone fragments were first aligned with a maximum gap of 2 mm, and these bone fragments were connected only through the combination of LCPs and screws. There was no contact between

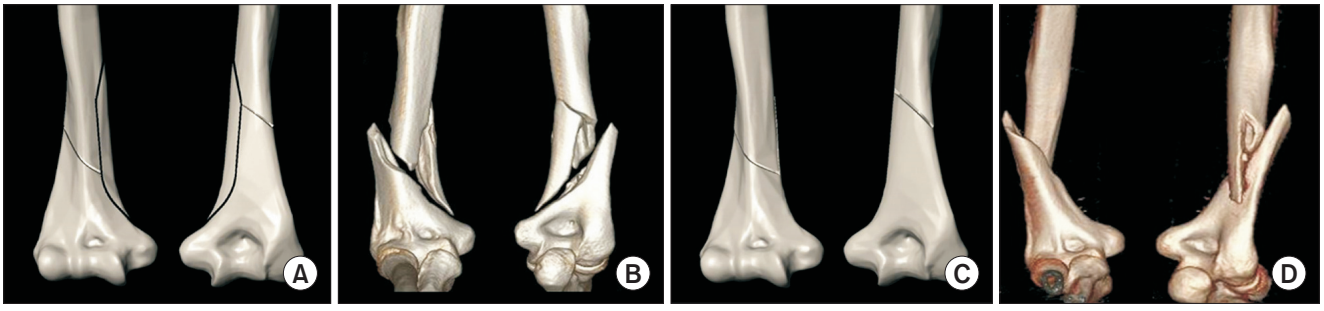

Fig. 2. Three-dimensional (3D) modeling of fracture models. (A) Three-part spiral wedge fracture (AO 12-B1) model in Solidworks. (B) Three-part spiral wedge fracture (AO 12-B1) model in patient's 3D computed tomography. (C) Two-part spiral fracture (AO 12-A1) model in Solidworks. (D) Two-part spiral fracture (AO 12-A1) model in patient's 3D computed tomography.

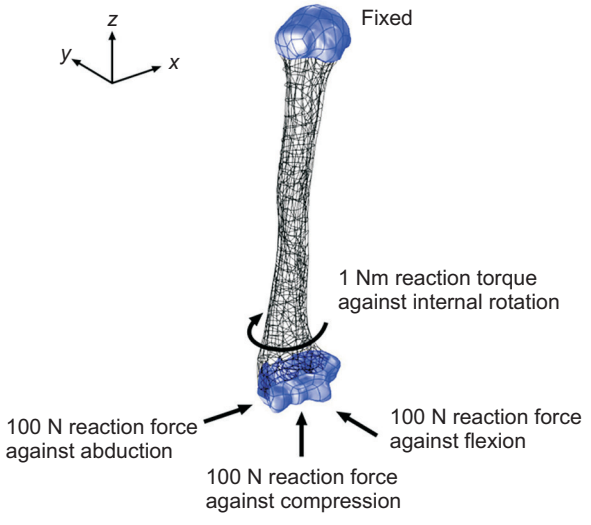

Fig. 3. Boundary conditions and loadings of finite element models.

Table 2. Numbers of Elements and Nodes and Degree of Freedom of Experiment Models

Model	Number of elements	Number of nodes	Degree of freedom
A	1,002,870	232,088	4,782,016
B	1,143,488	264,224	5,445,586
C	1,165,717	292,864	5,554,168
D	1,003,839	231,262	4,775,167
E	1,146,061	263,806	5,446,581
F	1,155,767	266,449	5,497,291
G	1,108,299	254,958	5,265,853
H	1,172,322	269,774	5,570,170

bone fragments in the initial configuration and in the configurations under the load in the subsequent FEA experiments.

Finite element analysis

The FEA experiment was conducted using COMSOL Multiphysics, a FEA, solver, and simulation software package (version 5.4, COMSOL Inc.). Fig. 3 shows the loading and boundary conditions used in the experiments. The virtual experiment environment was configured to match the biomechanical experiment environment in the real world, as previously reported.[17] In the simulator, the surface in contact with the upper humerus joint was attached to a rigid connector and fixed to a global frame. The surface in contact with the lower humerus joint was also attached to a rigid connector and received a load for each experiment model.

There were 4 types of loads: a torque of 1 Nm along the negative z-axis direction, simulating the reaction torque against internal rotation; a force of 100 N in the positive y-axis direction, simulating the reaction force against flexion; a force of 100 N in the positive z-axis direction, simulating the reaction force against compression; and a force of 100 N in the positive x-axis direction, simulating the reaction force against abduction.

Young's moduli for the cortical bone, titanium alloy LCPs, and titanium alloy screws were set to be 16.8 GPa, 110 GPa, and 110 GPa, respectively, based on previous FEA studies.[18] Poisson's ratios for all materials were set to be 0.3. Each experiment model was meshed with a 4-node tetrahedral 3D element. The number of elements, nodes, and degrees of freedom of each experiment model are shown in Table 2.

Clinical Study

Patient demographics

From July 2008 to February 2015, our group conducted a

clinical study that included 29 patients with DJFHs.[13] After that, we consistently applied the same ADPF procedure to DJFH patients from March 2015 to March 2021, resulting in 43 additional patients with DJFHs being operated on. In total, 72 patients were included in this study from both time periods. Exclusion criteria were follow-up of less than 1 year, pathologic fracture, revision surgery, and pediatric patients (Fig. 4).

By retrospectively reviewing medical records of the enrolled patients, we investigated patient demographics, injury mechanism, and AO classification of fracture. Patient demographic details included age, sex, sidedness, hand dominance, follow-up period, and operation time.

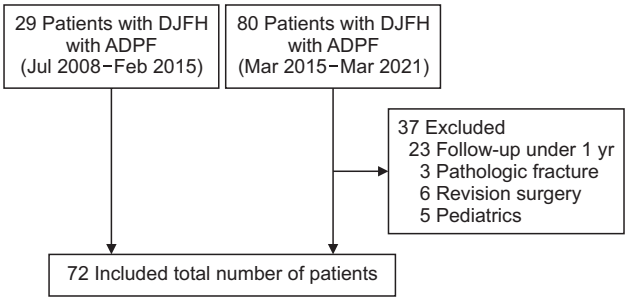

Fig. 4. Flowchart showing the slection of patients for the clinical study. DJFH: distal metaphyseal-diaphyseal junction fractures of the humerus, ADPF: anterolateral dual plate fixation.

We also investigated the occurrence of radial nerve palsy in the perioperative period and the removal of internal fixation after bone union.

Outcome measurement

Clinical results were evaluated by assessing elbow range of motion (ROM), Disabilities of the Arm, Shoulder and Hand (DASH) score, Mayo Elbow Performance Score (MEPS), and hand grip strength at the final follow-up. Grip strength was compared with the unaffected side, and a 7% correction was made according to dominance, referring to a previous study.[19] For radiographic results, alignment was determined by taking a long cassette view of the upper extremity to measure the elbow carrying angle. Fracture union was considered achieved when evidence of radiographic union became apparent. During the follow-up period, device removal surgery and complications were evaluated.

To investigate surgical instruments, 4.5-mm narrow LCP and 3.5-mm LCP (Depuy Synthes) were used in all surgeries. We also recorded the length of the plate used, the number of fixed screws, and the use of lag screws. Two independant orthopedic surgeons (1 senior resident [JO] and 1 junior resident [WA]) investigated patient's medical records and measured clinical outcomes. Conflicing data between the 2 investigators were determined by another

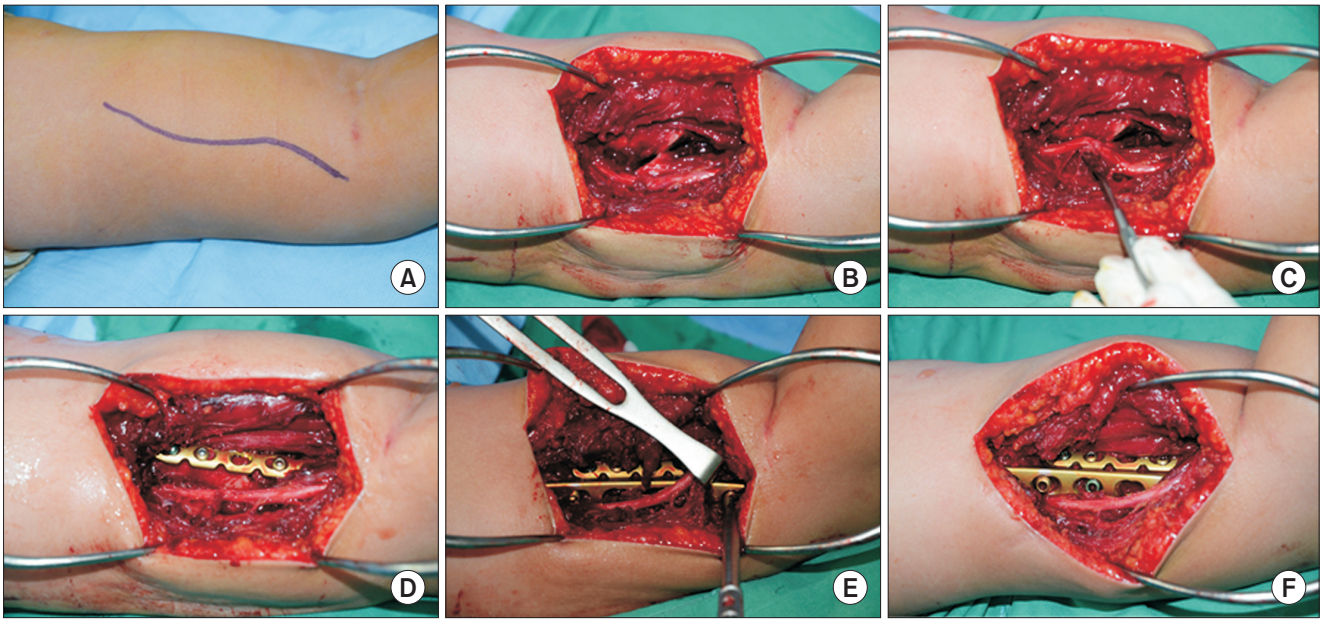

Fig. 5. Operative procedures through the anterolateral approach. (A) A skin incision was made along the lateral border of the biceps brachii. (B, C) The brachialis was split to expose the humerus, and the radial nerve was identified on the lateral aspect of the humerus. (D) A 3.5-mm locking compression plate (LCP) was applied on the anterior surface of the reduced humerus. (E, F) A 4.5-mm narrow LCP was applied to the humeral lateral cortex for definitive fixation.

orthopaedic specialist (JKL) as final data values. We used IBM SPSS ver. 23 (IBM Corp.) for statistical analysis.

Surgical procedures

All surgeries were performed by the same senior surgeon who specializes in upper extremity surgery (SHH). General anesthesia or regional brachial plexus block was used, and the operative elbow was extended to a radiolucent arm table in a supinated position with the patient in a supine position. A skin incision was made along the lateral border of the biceps brachii muscle over the fracture site. After dissection of the subcutaneous layer, the biceps brachii muscle was retracted medially, and the brachialis was split to expose the humerus. The radial nerve was identified on the lateral aspect of the humerus and protected. The fracture was reduced under direct visualization, and alignment was confirmed with portable image intensifiers.

A 3.5-mm LCP was applied to the anterior surface of the reduced humerus, with bone purchase near the cortex. In cases with a displaced fragment, 1 or 2 lag screws were inserted for better reduction. A 4.5-mm narrow LCP was applied to the humeral lateral cortex for definitive fixation. Due to the anatomic curvature, the plate was bent along the lateral border of the humerus. After checking for radial nerve impingement, the surgical wound was closed with a drain (Fig. 5).

After surgery, a Velpeau bandage was worn within 1 week. When the pain decreased immediately after surgery, ROM exercises for the elbow and shoulder were started as soon as possible. In cases of radial nerve palsy, a wrist extension splint was applied immediately after surgery, and wrist passive ROM exercises were performed. After stitches were removed, returning to daily activities was permitted at 2 weeks postoperatively. Follow-up was recommended at postoperative 2 weeks, 1, 2, 4, 6, and 9 months, and 1 year. Removal of the fixation device was conducted at 1 year postoperatively.

RESULTS

Finite Element Analysis

Structural stiffness

Table 3 presents the results of structual stiffness for all experimental models under 4 loading conditions. Fig. 6 displays the normalized stiffness results in comparion to those of the intact bone model. In all 4 loading conditions, models A and D with single plate fixation exhibited the lowest structural stiffness levels. Dual plate fixation provided greater structural stiffness than single plate fixation for both fracture models. Furthermore, dual fixation was found to be more effective in improving the structural stiffness of the B1 fracture than the A1 fracture (A vs. B and D vs. E). In particular, the dual fixation resulted in 41% higher torsional stiffness and 176% higher compressive stiffness than single fixation in the B1 fracture model.

It is worth noting that all fixation conditions provided high stiffness in anterior-posterior (A-P) bending and lateral-medial (L-M) bending. Models E, F, and G were able to restore the stiffness in A-P bending and L-M bending to the same extent as the intact model. However, none of the fracture fixation constructs fully restored the stiffness to the level of the intact model in torsion or compression. Therefore, the stiffness levels for these 2 loading conditions are well-suited to demonstrate the effectiveness of ADPF. Models B, C, E, and F with dual fixation exhibited superior results to models A and D with single fixation, suggesting that dual fixation could particularly improve structural stiffness in torsion and compression.

The comparison between models B and C models revealed that longer lengths of LCPs in the B1 fracture model reduced the overall structural stiffness, especially the stiffness in torsion and compression. As the plates become longer, the fixation locations between fractured bones tend to be further apart. Although the stiffness decreased due to the elongated LCPs, it remained higher than that of single plate fixation with a 7-hole LCP. Unlike the B1 fracture model. However, in the A1 fracture model, the length of LCPs did not appear to have a significant effect on structural stiffness since more screws were installed bicortically in the fracture model (E vs. F).

Table 3. Effective Structural Stiffness of Each Experiment Model under 4 Different Loading Conditions

Model	Torsional stiffness (Nm/rad)	Anteroposterior stiffness (N/mm)	Compressive stiffness (kN/mm)	Medial-lateral stiffness (N/mm)
Intact	248.0	18.0	3.12	19.6
A	66.1	15.0	0.78	14.9
B	93.9	16.9	2.17	18.5
C	70.8	15.9	1.32	17.5
D	102.7	14.3	1.16	18.5
E	125.5	17.9	2.28	19.5
F	100.8	18.5	2.32	20.5
G	70.9	16.0	1.59	17.9
H	141.1	18.3	2.76	19.8

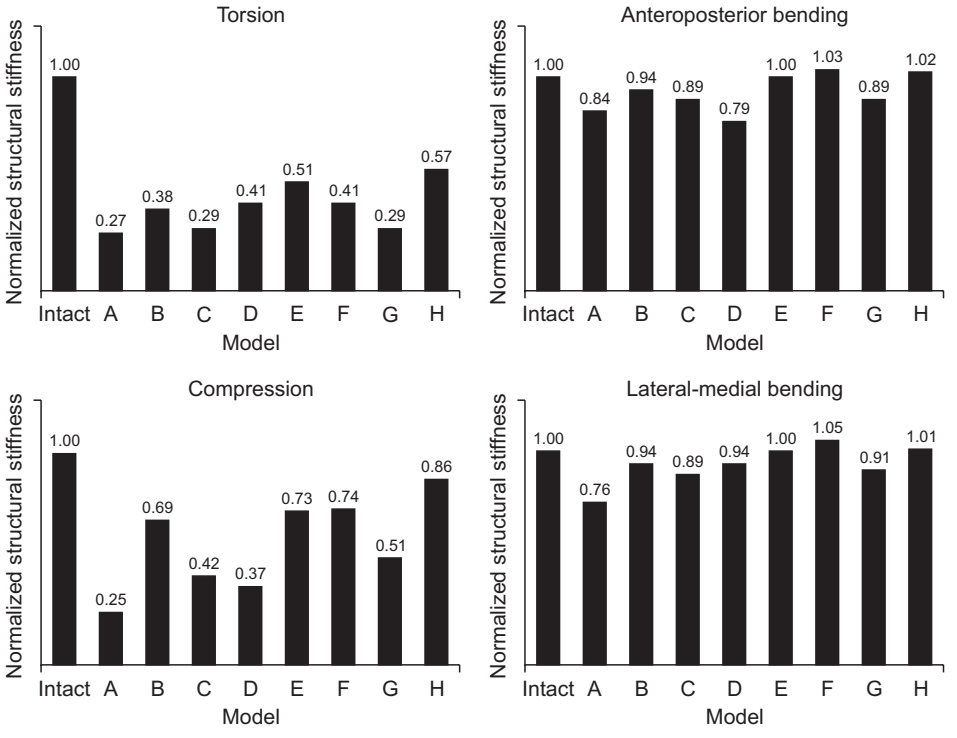

Fig. 6. Normalized structural stiffness levels of experimental models.

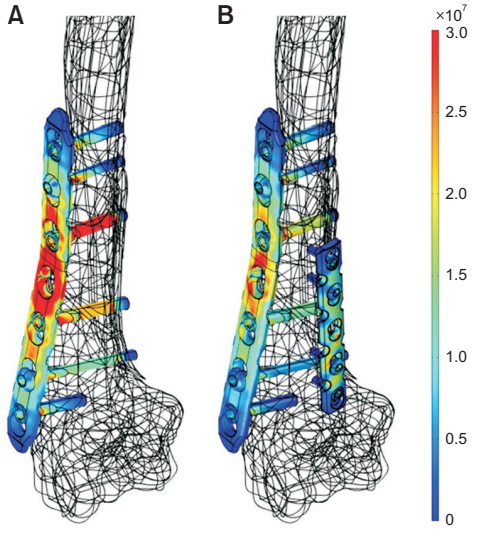

Fig. 7. Stress distributions of model A (A, single plate fixation) and model B (B, dual plate fixation) under a torsional load of 1 Nm.

The comparison between models E and G showed that the number of screws had a significant impact on the structural stiffness. Structural stiffness decreased under all loading conditions when a lateral LCP was installed with 4 screws. The torsional stiffness of model G was even lower than that of model D with a single plate fixation. Bicortical implantation of the anterior LCP also contributed to an increase in the structural stiffness (E vs. H). However, the

Table 4. Mean Stress of Locking Compression Plates of Experiment Models under 4 Different Loading Conditions

Model	Plate type	Mean stress on a torsional load (MPa)	Mean stress on a compressive load (MPa)	Mean stress on an antero-posterior load (MPa)	Mean stress on a medial-lateral load (MPa)
A	4.5 mm	9.90	4.90	42.9	26.8
B	4.5 mm	6.93	2.02	27.3	18.0
	3.5 mm	5.78	4.51	15.4	20.2
C	4.5 mm	9.23	4.59	39.6	25.3
	3.5 mm	9.21	8.43	34.1	40.3
D	4.5 mm	6.60	2.51	30.9	12.8
E	4.5 mm	5.39	1.96	25.2	12.7
	3.5 mm	5.22	4.43	16.9	13.9
F	4.5 mm	6.61	2.17	25.5	13.9
	3.5 mm	6.76	4.24	18.1	13.4
G	4.5 mm	9.95	3.72	35.2	17.3
	3.5 mm	10.80	7.70	39.5	32.7
H	4.5 mm	4.65	1.29	23.1	11.5
	3.5 mm	4.07	3.56	13.0	11.9

stiffness difference between the 2 models was small when considering other control parameters such as the number of plates, lengths of plates, and the number of screws.

Plate stress distribution

Fig. 7 visualizes stress distributions of single fixation and dual fixation under a torsional load of 1 Nm. It was observed that the stress distributed across the LCP with dual fixation was lower than that across the LCP with single fixation. In the case of dual fixation, the mean stress values in the anterior and lateral plates were 42% and 30% lower than those in the plate with single fixation as the dual plates shared the external torsional load.

Table 4 shows the mean stress of all experimental models under the 4 loading conditions, while Fig. 8 shows the mean stress of LCPs with dual fixation normalized by the mean stress of LCPs with single fixation for each fracture model. Overall, the addition of the anterior plate lowered the mean stress in the lateral plate, implying that dual fixation could withstand a greater load than single fixation without plastic deformation. As the length of the LCP increased, the mean stress on the LCP tended to increase. The mean stress in the lateral 2-screw model G was much higher than that of the single plate. A lower number of screws not only decreased the overall structural stiffness but also increased the stress in the LCP, thereby increasing the possibility of plastic deformation or cracking of the LCP.

In FEA simulation, dual fixation models (with 7-hole and 5-hole or with 8-hole and 6-hole) showed higher structural stiffness with lower stress than a single plate. The stiffness and stress results also suggest that at least 3 screws (6 cortices) must be inserted into the lateral plate to effectively reduce the external load.

Clinical study

The study included patients with an average age of 38.7 years, with a higher prevalence of men (69.4%), right side (55.5%), and dominant arm (58.3%). The most common mechanisms of injury were traffic accidents (36.1%) and fall downs (33.3%), with arm wrestling being the most common cause of sports injuries (20.8%). The most frequent fracture types were B1 spiral wedge fracture (33.3%) and A1 spiral fracture (29.2%). The average follow-up period was 24.5 months (Table 5).

Regarding clinical results of surgery, patients showed satisfactory results in terms of ROM, with good elbow flexion, elbow extension, and forearm rotation. The average DASH score was 4.3 and the average MEPS was 88.2. The average grip power was 49.2 kg, which was 96% of that of the unaffected side. Radiographic results showed an average carrying angle of 168.6° and a mean time to bony union of 8.7 weeks. Implant removal was performed in 31 patients (43%), with a mean removal time of 14.5 months postoperatively (Table 6, Fig. 9).

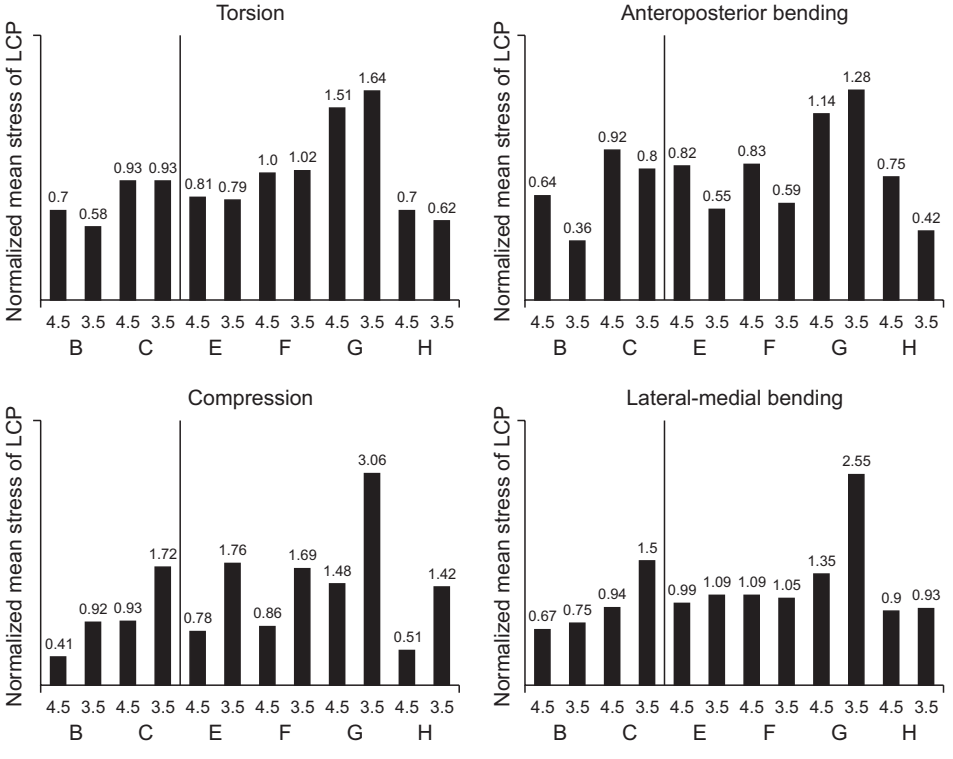

Fig. 8. Normalized mean stress of locking compression plates (LCPs). B and C are normalized by A. E-H are normalized by D.

Table 5. Demographics of Enrolled Patients

Demographics	Value
Age (yr)	38.7 (17–94)
Sex (male : female)	50 : 22
Sidedness (right : left)	40 : 32
Dominant arm	42 (58.3)
Injury mechanism	
Traffic accident	26 (36.1)
Sports injury except arm wrestling	7 (9.7)
Arm wrestling	15 (20.8)
Fall down	24 (33.3)
AO/OTA classification	
A1	21 (29.2)
A2	8 (11.1)
A3	6 (8.3)
B1	24 (33.3)
B2	6 (8.3)
B3	5 (6.9)
C	2 (2.7)
Operation time (min)	55.1 (34–105)
Follow-up period (mo)	24.5 (12–106)

Values are presented as mean (range) or number (%).
OTA: Orthopaedic Trauma Association.

Table 6. Postoperative Outcomes Including Clinical Scores and Radiologic Results

Postoperative outcome	Value
Clinical score	
Range of motion (°)	
Elbow flexion	138.3 ± 12.5
Elbow extension	2.5 ± 6.7
Forearm supination	77.6 ± 5.4
Forearm pronation	74.5 ± 4.5
DASH score	4.3 ± 10.9
MEPS	88.2 ± 17.8
Grip power (kg)	49.2 (96)*
Grip power contralateral hand (kg)	51.6
Radiologic result	
Carrying angle (°)	168.6 ± 11.4
Time to union (wk)	8.7 ± 6.5
Device removal	31 (43)
Time to device removal (mo)	14.5 (12–47)

Values are presented as mean ± standard deviation or mean (range) unless otherwise indicated.
DASH: Disabilities of the Arm, Shoulder and Hand, MEPS: Mayo Elbow Performance Score.
*The average grip power was 49.2 kg, which was 96% of that of the unaffected side.

Radial nerve palsy was observed in 9 and 2 patients during the preoperative and postoperative periods, respectively. All motor functions recovered within 6 months without sequelae, but chronic tingling sensation persisted in 2 cases. No surgical treatment for radial nerve exploration or neurolysis was performed (Table 7).

As for fixation devices, the 7-hole length (51.4%) was the most commonly used for the 4.5-mm LCP, followed by the 8-hole length (25%). For the 3.5-mm LCP, the 5-hole length (58.3%) was the most commonly used. Lag screws were used in 20 cases (27.8%) (Table 8).

DISCUSSION

In this study, we demonstrated the efficacy of using ADPF for DJFH through a biomechanical study using FEA and the clinical results of 72 patients simultaneously. Previous biomechanical FEA studies have only demonstrated the efficiency of double plate fixation in distal intra-articular humerus fractures or mid-shaft humerus fractures,[15,20] but no biomechanical studies have been conducted on DJFH. Moreover, earlier studies on the humerus midshaft presented a simple transverse 2-fragment fracture as the only fracture model,[15] whereas our study introduced a spiral fracture model and a 3-fragment butterfly wedge fracture model. As humerus fracture is more frequently caused by rotational mechanism, there are more cases with a spiral fracture line than with a transverse fracture caused by a direct blow. Therefore, these models are more common patterns of DJFH. This was also shown in the results of our clinical study, where B1 and A1 were the 2 most common classifications, each accounting for about 30%.

Most finite element studies did not distiguish between cortical screws and locking screws, leading to a severe lack of realism.[20,21] In our study, we simulated the fracture construct models more realistically by dividing how cortical screws and locking screws acted differently. Although other previous FEA studies have investigated the

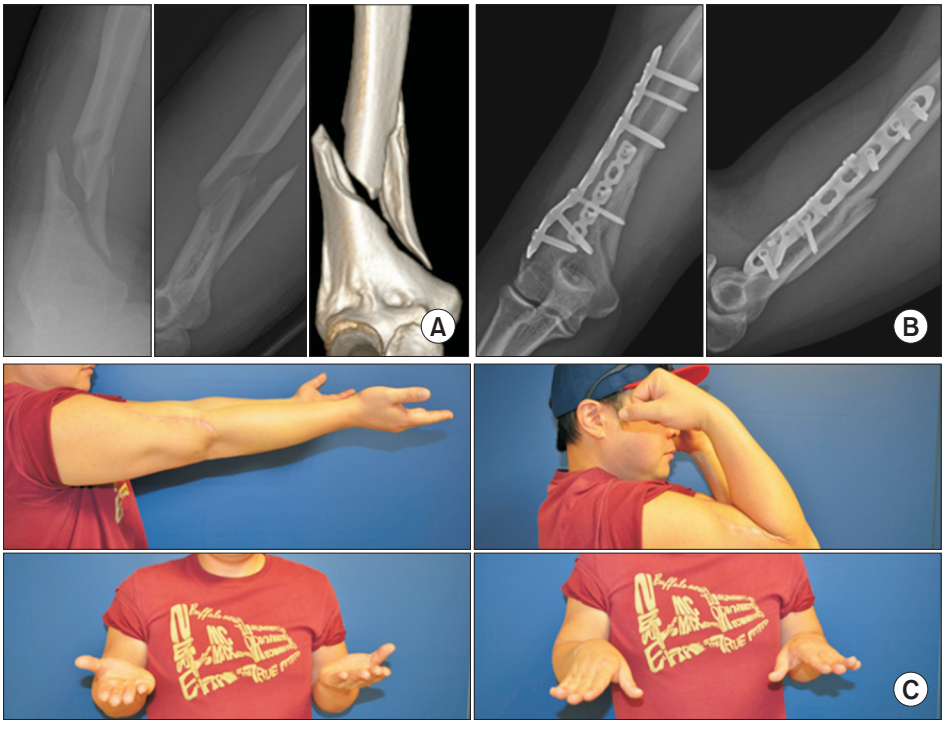

Fig. 9. Clinical outcomes of surgical treatment in a 34-year-old man with a distal junctional fracture of the humerus. (A) Preoperative plain radiography and 3-dimensional computed tomography. (B) Postoperative 3-month radiographs showing achievement of bony union. (C) Range of motion showing satisfactory results.

Table 7. Accompanied Radial Nerve Symptoms

Preoperative	Postoperative	Persisted more than 6 months	Operative treatment
9 (12.5)	2 (2.8)	Sensory: 2 (2.8) Motor: 0	0

Values are presented as number (%).

Table 8. Fixation Device Used for Surgery

Plate length	No. (%)
4.5-mm narrow LCP	
6-Hole	3 (4.2)
7-Hole	37 (51.4)
8-Hole	18 (25)
9-Hole	9 (12.5)
10-Hole	5 (6.9)
3.5-mm reconstruction plate	
4-Hole	4 (5.6)
5-Hole	42 (58.3)
6-Hole	24 (33.3)
7-Hole	2 (2.8)
Lag screw	20 (27.8)
1	11
2	9

LCP: locking compression plate.

effect of dual plate fixation for clavicle fracture and periprosthetic femur fracture,[21] only simple transverse models were implemented. Additionally, it is difficult to apply the dual-plate methods in the real field because it requires additional incisions or approaches. In our anterolateral approach, the dual plate was easily applicable in the surgical field through 1 approach.

A total of 8 models were analyzed to provide solutions to various clinical questions during surgery. The dual plate fixation method showed higher structural stiffness in all 4 loads for both fracture models compared to the single plate fixation method, as indicated by the comparisons of the results of models A and D with the results of models B and E, respectively. The maximum value of enhanced stiffness was observed under compressive load for both B1 and A1 fracture models, with an increase of 176% and 97%, respectively. The minimum values of enhanced stiffness were 11% for A-P bending in the B1 fracture model and 6% for L-M bending in the A1 fracture model.

For the spiral wedge fracture, longer LCPs tended to provide lower structural stiffness and higher stress in plates. However, this tendency was not significantly visible

in models with a spiral fracture, indicating that other parameters such as the number of cortices of the lateral plate and the location of LCPs on the bone also contribute to structural stiffness.

The FEA results of model G highlighted the importance of the number of cortices. In model G, which only had 2 screws inserted at each side of the lateral plate, a total of 4 screws showed even lower stiffness than the single plate model D in torsion and L-M bending and higher stress in LCPs. Therefore, even if dual plate fixation is applied during surgery, at least 3 screws should be inserted into the main lateral plate. More attention should be paid to the torsional load if sufficient cortex purchasing is not obtained due to the fracture pattern.

Finally, model H was used to determine whether it was necessary to hold the far cortex on the 3.5-mm anterior plate. The results showed that the stiffness was similar to that of the model in which only the near cortex was purchased. Therefore, the anterior plate could obtain sufficient strength only with near cortex fixation.

To conclude the FEA study, all combinations (7-hole with 5-hole and 8-hole with 6-hole) showed generally superior performances than a single plate, and at least 3 screws (6 cortices) should be inserted into the lateral plate to reduce the load effectively. For the anterior plate, it was sufficient to purchase only the near cortex. A considerable portion of humerus fractures occur due to rotational injuries, resulting in a high incidence of spiral pattern fractures. Following dual plate fixation, better resistance against torsional forces was achieved.

Although models used in this FEA study had large enough number of elements in meshing to increase the accuracy in results, there were some assumptions made for efficient computing that might have produced results different from actual biomechanical results. First, it allows only for comparison among various fixation options, albeit without establishing an absolute value of "sufficient stiffness." Second, the trabecular bone in the humerus was not considered as its Young's modulus was considerably lower than that of the cortical bone.[22] Lastly, the bone-screw interface was not fully realistically implemented. The interface was implemented using cylindrical screws based on the results from previous studies that the global load-deformation response is not significantly influenced by a specific screw-bone interface.[23,24]

In the clinical field, there have been previous attempts to treat fractures using multiple plates for a long time. The concept of a "reduction plate" was used as a temporary reduction aid until a definitive fixation could be introduced. Many reports have utilized dual plating to aid in fracture fixation.[25] When examining the use of dual plating specifically for the humerus, studies have applied it to proximal and distal intra-articular fractures.[6,26] In particular, for distal intra-articular fractures, dual plating has become a popular standard procedure based on the 2-column theory. Recently, fixation using dual plates for both anterolateral and posterior approaches has been reported for DJFH.[7,13] Both studies reported good outcomes, although the numbers of patients included were relatively small.

Various approaches and fixation devices have been used to treat DJFH. The method using the minimally invasive percutaneous plate (MIPO) technique and an extra-articular distal humerus plate, also known as a "hockey stick plate," has been the most commonly used method.[27,28] However, the MIPO technique is not considered suitable for fractures in the DJFH due to the risk of radial nerve entrapment and concave curvature. Skin irritation and possible impingement on the olecranon fossa are also potential problems for hockey stick plates.[28]

Recently, novel techniques using the reversed Philos plate or intramedullary nailing have been introduced.[11] The application of the reversed Philos plate is a clever idea, but it is for out-of-label use. In addition, it is impossible to fix fractures beyond the olecranon fossa. Additionally, metal failure is a risk with 3.5-mm screws.[11] In the case of nailing, distal fixation is impossible at the junctional level, and only 1 hole can be used without a locking mechanism.

The anterolateral approach utilized in this study offers several advantages.[13] First, it can be performed with the patient in a neutral supine position, allowing the surgeon to operate comfortably in a stable sitting position. Furthermore, a brachial plexus block can be administered if necessary, and the preparation time for surgery is relatively short. Additionally, the approach results in a small, less visible scar.

Direct visualization of the radial nerve during surgery can also be advantageous, as approximately 20% of patients experience preoperative neurological symptoms or paralysis. The rate of postoperative paralysis is as high as 10%.[29,30] Therefore, it is safer for the patient and the surgeon to visually inspect the radial nerve during surgery and perform neurolysis if necessary. In our clinical results, 9 patients (12.5%) experienced radial nerve palsy preoperatively, while 2 patients (2.8%) developed the condition postoperatively. All motor functions recovered within 6 months with conservative treatment, including physical therapy and bracing.

Although this study included a relatively large number of patients, it is limited by its retrospective design and

lack of a comparison group. However, all surgeries were performed by a single experienced surgeon on consecutive patients, which minimized confounding factors. ADPF was biomechanically superior to the single plate method in FEA of the DJFH model. ADPF was also clinically effective in a large cohort of DJFH.

CONFLICT OF INTEREST

No potential conflict of interest relevant to this article was reported.

ACKNOWLEDGEMENTS

This work was supported by an AO Trauma Asia Pacific Research Grant (AOTAP-2022-04).

ORCID

Cheungsoo Ha https://orcid.org/0000-0003-2027-0625
Inrak Choi https://orcid.org/0000-0002-5102-7209
Jun-Ku Lee https://orcid.org/0000-0003-4640-9357
Jongbeom Oh https://orcid.org/0000-0003-1687-3730
Wooyeol Ahn https://orcid.org/0000-0001-5664-222X
Soo-Hong Han https://orcid.org/0000-0002-8951-650X

REFERENCES

1. Igbigbi PS, Manda K. Epidemiology of humeral fractures in Malawi. Int Orthop. 2004;28(6):338-41.
2. Tytherleigh-Strong G, Walls N, McQueen MM. The epidemiology of humeral shaft fractures. J Bone Joint Surg Br. 1998;80(2):249-53.
3. Toivanen JA, Nieminen J, Laine HJ, Honkonen SE, Jarvinen MJ. Functional treatment of closed humeral shaft fractures. Int Orthop. 2005;29(1):10-3.
4. Jawa A, McCarty P, Doornberg J, Harris M, Ring D. Extra-articular distal-third diaphyseal fractures of the humerus: a comparison of functional bracing and plate fixation. J Bone Joint Surg Am. 2006;88(11):2343-7.
5. Lee SK, Yang DS, Chang SH, Choy WS. LCP metaphyseal plate fixation for fractures of the distal third humeral shaft using brachialis splitting approach. Acta Orthop Belg. 2016;82(1):85-93.
6. Shin SJ, Sohn HS, Do NH. A clinical comparison of two different double plating methods for intraarticular distal humerus fractures. J Shoulder Elbow Surg. 2010;19(1):2-9.
7. Prasarn ML, Ahn J, Paul O, et al. Dual plating for fractures of the distal third of the humeral shaft. J Orthop Trauma. 2011;25(1):57-63.
8. Swellengrebel HJ, Saper D, Yi P, Weening AA, Ring D, Jawa A. Nonoperative treatment of closed extra-articular distal humeral shaft fractures in adults: a comparison of functional bracing and above-elbow casting. Am J Orthop (Belle Mead NJ). 2018;47(5).
9. Ekholm R, Ponzer S, Tornkvist H, Adami J, Tidermark J. The Holstein-Lewis humeral shaft fracture: aspects of radial nerve injury, primary treatment, and outcome. J Orthop Trauma. 2008;22(10):693-7.
10. Kharbanda Y, Tanwar YS, Srivastava V, Birla V, Rajput A, Pandit R. Retrospective analysis of extra-articular distal humerus shaft fractures treated with the use of pre-contoured lateral column metaphyseal LCP by triceps-sparing posterolateral approach. Strategies Trauma Limb Reconstr. 2017;12(1):1-9.
11. Sohn HS, Shin SJ. Modified use of a proximal humeral internal locking system (PHILOS) plate in extra-articular distal-third diaphyseal humeral fractures. Injury. 2019;50(7):1300-5.
12. Jitprapaikulsarn S, Neti N, Thremthakanpon W, Gromprasit A. Anterior minimally invasive plating osteosynthesis using reversed proximal humeral internal locking system plate for distal humeral shaft fractures. Eur J Orthop Surg Traumatol. 2020;30(8):1515-21.
13. Lee JK, Choi YS, Sim YS, Choi DS, Han SH. Dual plate fixation on distal third diaphyseal fracture of the humerus. Int Orthop. 2017;41(8):1655-61.
14. Lewis GS, Mischler D, Wee H, Reid JS, Varga P. Finite element analysis of fracture fixation. Curr Osteoporos Rep. 2021;19(4):403-16.
15. Kosmopoulos V, Luedke C, Nana AD. Dual small fragment plating improves screw-to-screw load sharing for mid-diaphyseal humeral fracture fixation: a finite element study. Technol Health Care. 2015;23(1):83-92.
16. Mitsuhashi N, Fujieda K, Tamura T, Kawamoto S, Takagi T, Okubo K. BodyParts3D: 3D structure database for anatomical concepts. Nucleic Acids Res. 2009;37(Database issue):D782-5.
17. Ahmad M, Nanda R, Bajwa AS, Candal-Couto J, Green S, Hui AC. Biomechanical testing of the locking compression plate: when does the distance between bone and implant significantly reduce construct stability? Injury. 2007;38(3):358-64.

18. Mei J, Liu S, Jia G, Cui X, Jiang C, Ou Y. Finite element analysis of the effect of cannulated screw placement and drilling frequency on femoral neck fracture fixation. Injury. 2014;45(12):2045-50.
19. Kim M, Won CW, Kim M. Muscular grip strength normative values for a Korean population from the Korea National Health and Nutrition Examination Survey, 2014-2015. PLoS One. 2018;13(8):e0201275.
20. Kong L, Wang Y, Lu Q, Han Y, Wang F. Biomechanical properties of a novel fixation system for intra-articular distal humerus fractures: a finite element analysis. J Orthop Surg Res. 2021;16(1):674.
21. Zhang F, Chen F, Qi Y, et al. Finite element analysis of dual small plate fixation and single plate fixation for treatment of midshaft clavicle fractures. J Orthop Surg Res. 2020;15(1):148.
22. Rho JY, Ashman RB, Turner CH. Young's modulus of trabecular and cortical bone material: ultrasonic and microtensile measurements. J Biomech. 1993;26(2):111-9.
23. MacLeod AR, Pankaj P, Simpson AH. Does screw-bone interface modelling matter in finite element analyses? J Biomech. 2012;45(9):1712-6.
24. Moazen M, Mak JH, Jones AC, Jin Z, Wilcox RK, Tsiridis E. Evaluation of a new approach for modelling the screw-bone interface in a locking plate fixation: a corroboration study. Proc Inst Mech Eng H. 2013;227(7):746-56.
25. Archdeacon MT, Wyrick JD. Reduction plating for provisional fracture fixation. J Orthop Trauma. 2006;20(3):206-11.
26. Choi S, Kang H, Bang H. Technical tips: dualplate fixation technique for comminuted proximal humerus fractures. Injury. 2014;45(8):1280-2.
27. Ji F, Tong D, Tang H, et al. Minimally invasive percutaneous plate osteosynthesis (MIPPO) technique applied in the treatment of humeral shaft distal fractures through a lateral approach. Int Orthop. 2009;33(2):543-7.
28. Scolaro JA, Voleti P, Makani A, Namdari S, Mirza A, Mehta S. Surgical fixation of extra-articular distal humerus fractures with a posterolateral plate through a triceps-reflecting technique. J Shoulder Elbow Surg. 2014;23(2):251-7.
29. Shao YC, Harwood P, Grotz MR, Limb D, Giannoudis PV. Radial nerve palsy associated with fractures of the shaft of the humerus: a systematic review. J Bone Joint Surg Br. 2005;87(12):1647-52.
30. Schwab TR, Stillhard PF, Schibli S, Furrer M, Sommer C. Radial nerve palsy in humeral shaft fractures with internal fixation: analysis of management and outcome. Eur J Trauma Emerg Surg. 2018;44(2):235-43.